IEEE Access
Multidisciplinary ⋮ Rapid Review ⋮ Open Access Journal

Received October 21, 2019, accepted November 28, 2019, date of publication December 19, 2019, date of current version January 9, 2020.

Digital Object Identifier 10.1109/ACCESS.2019.2960873

CRowNet: Deep Network for Crop Row Detection in UAV Images

MAMADOU DIAN BAH[1], ADEL HAFIANE[2], AND RAPHAEL CANALS[1]
[1]University of Orleans, PRISME, EA 4229, F45072 Orleans, France
[2]INSA Centre Val de Loire, PRISME, EA 4229, F180222 Bourges, France

Corresponding author: Mamadou Dian Bah (m-dian.bah@univ-orleans.fr)

This work was supported by the ADVENTICES Project through the Centre-Val de Loire Region (France) under Grant ADVENTICES 16032PR.

ABSTRACT Nowadays, the development of robots and smart tractors for the automation of sowing, harvesting, weeding etc. is transforming agriculture. Farmers are moving from an agriculture where everything is applied uniformly to a much more targeted farming. This new kind of farming is commonly referred to as precision agriculture. However for autonomous guidance of these agricultural machines and even sometimes for weed detection an accurate detection of crop rows is required. In this paper we propose a new method called CRowNet which uses a convolutional neural network (CNN) and the Hough transform to detect crop rows in images taken by an unmanned aerial vehicle (UAV). The method consists of a model formed with SegNet (S-SegNet) and a CNN based Hough transform (HoughCNet). The performance of the proposed method was quantitatively compared to traditional approaches and it showed the best and most robust result. A good crop row detection rate of 93.58% was obtained with an *IoU* score per crop row above 70%. Moreover the model trained on a given crop field is able to detect rows in images of different types of crops.

INDEX TERMS Crop row detection, deep learning, weed detection, Hough transform, image processing.

I. INTRODUCTION

Currently, losses due to pests, diseases and weeds can reach 40% of global crop yields each year and this percentage is expected to increase significantly in the coming years [1]. In order to reduce the amount of chemicals while continuing to increase productivity, the concept of precision agriculture was introduced [2], [3]. Precision agriculture can be defined as the application of technology for the purpose of improving crop performance and environmental quality [2]. The main goal of precision agriculture is to implement the right management practice in order to allocate the right doses of inputs such as fertilizers, herbicides, seed, fuel, etc. to the right place and at the right time [4]. However all the aforementioned processes require accurate guidance with respect to crop rows. Some studies showed the interest of the automation of crop row detection for robot navigation [5]–[7], and also for the detection of weeds between rows [8], [9]. In the literature different imaging-based methods have been used for detecting crop rows. Typically, these methods fall into a few categories according to their detection principle, such as Hough transform, linear regression, blob analysis, stereo vision, and horizontal strips. However, these methods do not take into account the advantages of a deep learning approach.

Recently, convolutional neural networks (CNNs) have emerged as a powerful approach for computer vision tasks. The first major success of CNNs [10] was achieved on the ImageNet Large Scale Vision Recognition Challenge 2012 (ILSCVR12) with the AlexNet network [11]. AlexNet showed that a large, deep convolutional neural network is capable of achieving record-breaking results on a highly challenging dataset using purely supervised training. Nowadays, deep learning is becoming a powerful approach in several domains to solve many big data problems such as computer vision, speech recognition, and natural language processing. In agriculture, CNNs have been used for different problems such as weed detection, plant classification, plant disease detection but not for crop row detection [12]–[17].

In this paper we propose a new method that combines CNN and the Hough transform to extract crop rows in images taken by an unmanned aerial vehicle (UAV). The aim is to design a robust method able to detect and highlight the crop rows.

The paper is divided into four parts. In section 2 we discuss related work. Section 3 presents the proposed method.

The associate editor coordinating the review of this manuscript and approving it for publication was Sotirios Goudos.

In section 4 we present and discuss the experimental results obtained. Section 5 concludes the paper.

II. RELATED WORK

The Hough transform [18] is one of the most commonly used machine vision methods for identifying crop rows. It was used to guide mobile robots in sugar beet and rapeseed fields in [19]. With extensive field tests the authors showed that the system was accurate and fast enough to control a weeder and a mobile closed-loop robot with a standard deviation of the position of 2.7 and 2.3 cm, respectively. The Hough transform was used to detect curves and straight lines in [20]. Baker *et al.* [21] applied the Hough transform to extract crop rows from images acquired by a robot using a specific angle interval. They assumed that the position of the robot in relation to the crop rows was greater than 45°. Thus the Hough transform was computed over an angle range from 45° to 135° with a step of 1°. In [8], Excess Green Index (ExG) [22] and Otsu thresholding [23] helped to remove the background (soil, residues) before performing a double Hough transform to identify the crop rows in perspective images. Jones *et al.* [24] detected crop rows by modeling agronomic images taken from a virtual camera placed in a virtual field with and without perspective. However, despite the effectiveness of the Hough transform, the method has some shortcomings, such as the computation time required and also its sensitivity in images with a high weed pressure. Ji and Qi [25] proposed RHT (Random Hough Transform) [26] to detect crop rows. The particularity of RHT is that the Hough transform is applied to randomly selected vegetation pixels. Compared to the Hough transform, about 45% of processing time is saved. Bah *et al.* [27] used the Hough transform and Simple Linear Iterative Clustering (SLIC) to detect crop rows. After Hough transform computation the biggest challenge was to select the lines that best go through the center of crop rows due to the inter-row weeds and the width of crop rows. Gee *et al.* [8] proposed to exploit the parallelism of crop rows and also the prior knowledge about inter-row distance. Parallelism makes it possible to hypothesize that if the crop rows are parallel in the image space, the votes of these rows will be aligned around the angle corresponding to the overall orientation. In addition, these votes are separated by a distance equivalent to the inter-row space. Thus, to extract the main lines of each crop row, Gee *et al.* identified the first maximum and then with a step corresponding to the theoretical interline distance they moved on either side of this maximum to retrieve the other maximum. This method has proven to be effective in detecting crop rows with a constant inter-row distance and constant orientation. In real agricultural fields, however, the imperfection of the soil and the presence of tractor tracks, mean that the rows are not always straight, parallel, and equidistant. In view of these different challenges, we proposed in [27] to use a ''pick and delete'' process. In the remainder of this paper we will refer to this method as ''CR-Hough-SLIC''. It consists in using superpixels generated by SLIC to detect only one line per crop row in order to avoid the impact of weeds. However, this method requires defining the number of superpixels and skeletons of the vegetation as input. For an image with N crop rows at least $N + 1$ Hough transforms will be calculated; the first one corresponds to the Hough transform computed on all the skeletons of the crop rows and the N others correspond to the Hough transform calculated on the superpixels of each line.

Some authors have preferred to use linear regression to detect crop rows, assuming that each crop row is a cloud of points that can be fitted by a line. Søgaard and Olsen [28] located the crop rows in a barley field using a weighted linear regression. In their experiments they showed that depending on the level of growth it was possible to detect the crop rows with an accuracy from ± 6 mm to ± 12 mm. Hague *et al.* [29] determined the position and orientation of crop rows by applying the non-linear version of the Kalman filter called extended Kalman filter [30]. Montalvo *et al.* [31] proposed to use linear regression to detect crop rows in a maize field with a high weed pressure. The analysis of spots or blobs is a fundamental technique in computer vision, based on the analysis of image regions that present a certain visual coherence. Fontaine and Crowe [32] relied on the direction and center of gravity of the different blobs to propose a crop row detection method. Burgos-Artizzu *et al.* [6] using a combination of the centre of gravity, the direction of blob regions and the direction of movement of a tractor with a camera mounted on it, proposed methods to detect crop rows. Pena *et al.* [9] developed an object-by-object image analysis (OBIA) procedure on a series of UAV images for the automatic discrimination of crop rows and weeds in a corn field. They segmented images into homogeneous superpixel objects. Thus, with a large scale they highlighted the structures of the crop rows and with the small scale they highlighted the objects within the crop rows. The authors found that the process is strongly influenced by the presence of weeds in close to or within crop rows. In [33], [34] the authors located the crop rows with an altimetric map of the field. But this method is generally used in cases where the plant heights are sufficiently large.

In agriculture, CNNs were applied to classify patches of water hyacinth, serrated tussocks and tropical soda apple in [17]. Mortensen *et al.* [16] used CNNs for semantic segmentation in the context of mixed crops on images of an oil radish plot trial with barley, grass, weeds, stumps and soil. Milioto *et al.* [35] achieved accurate weed classification in real sugar beet fields with mobile agricultural robots. Dos Santos Ferreira *et al.* [36] applied AlexNet for the detection of weeds in soybean crops. Bah *et al.* [13], used CNN for weed detection in different crop fields such as beet, spinach and bean in UAV imagery. Kerkech *et al.* [15] identified symptoms in grape leaves with CNN and color information.

Overall, traditional deep learning algorithms have proven to be effective for classification and semantic segmentation, but very few have been designed to study the spatial relationship of pixels on the rows and columns of an image. The most fully developed methods for long and continuous strip pattern

segmentation with CNN are applied to traffic lane and road detection in order to improve autonomous driving. In [37] a method called SCNN (Spatial CNN) was proposed to detect long structures or large objects with strong spatial relationships including traffic lanes, poles and also walls. In [38], [39] the authors used recurrent neural networks (RNN) to transmit information along each row or column, so that in the RNN layer each pixel position could only receive information from the same row or column. In [40] a network called StripNet was proposed to segment long and continuous strip patterns in different image modalities. In [41] the authors combined lane detection with vanishing point prediction to enhance the learning of context information, and proposed a network called Vpgnet. CNN with a Markov random field (MRF) was used for road detection in [42]. In general, the methods applied for road lane detection are designed to detect up to 4 lanes, whereas in the case of UAV images acquired in an agricultural field, the number of rows in an image can be more than 10 depending on the spatial resolution of the camera, the flight altitude and also the distance between crop rows. Moreover, the crop rows are close to each other and can be confused by inter row weeds or the dense vegetation. Therefore, the state of the art methods based on CNN may fail, because they were not designed for this particular problem.

We generally have two types of information in agricultural images acquired by UAV, the background (soil, rocks, etc.) and the vegetation (crop, weeds). Our work is motivated by the fact that while existing studies have focused on using semantic segmentation with CNNs such as SegNet and FCN for crop, weeds and background segmentation, none, to the best of our knowledge, have applied it to detecting and highlighting crop rows.

III. METHOD

We propose an approach that uses a fully convolutional network for crop row detection. It is based on two different architectures, the S-SegNet and the HoughCNet. The overall structure of the method is presented in Fig. 1. As input the method takes an RGB image, and using the S-SegNet, strips corresponding to the crop rows are extracted. The S-SegNet provides strips with smooth contours and reduces the impact of sowing errors by attaching the discontinuous rows. However, it is less robust against the strong presence of weeds in the inter-row space. S-SegNet is therefore accompanied by the HoughCNet whose purpose is to adjust the strips impacted by weeds. HoughCNet uses the Hough transform and CNN to extract the pixels that form the longest lines in the image. Small lines caused by the presence of inter-row weeds are eliminated. To ensure that noise has not been added by the HoughCNet, an intersection is applied between its output and that of the S-Segnet. At the end of this intersection it is generally observed that there are some discontinuities or that the strips obtained are not smooth. Thus, the S-SegNet is applied again to adjust these strips. Depending on weed pressure, this operation is applied once or several times. Therefore we used a loop based on the IoU (intersection over union) score. The loop is stopped when the IoU between the S-SegNet and the adjusted output (HoughCNet + Intersection + S-SegNet) is high ($IoU > \epsilon$).

A. S-SEGNET

In the state of the art presented above, we saw that recently various studies have been proposed to segment vegetation (crops and weeds) and soil with or without deep learning algorithms. However, all these studies seek to segment the plants individually to obtain a result that best fits the contours of these plants. Subsequently, this segmentation is used for other applications, such as extracting crop rows to guide robots or detecting weeds between rows. In the present study, the combination of vegetation segmentation and crop row detection is proposed in a single step. The purpose of S-SegNet is to detect strips (crop rows) with an RGB image as input and SegNet.

SegNet [43] is a deep fully convolutional neural network for semantic segmentation. Basically it was designed for scene understanding applications. It is therefore designed to be both efficient in terms of memory and computation time when inferring. In addition, the number of parameters to be driven is also very small and can be trained from end-to-end with a stochastic gradient descent. One advantage of using a deep fully convolutional neural network is that images of arbitrary size can be input to the network and a segmentation map of the same size can be obtained.

The SegNet architecture is composed of encoders, decoders and a pixel classification layer. Its particularity is that each encoder has its corresponding decoder. Encoders are generally convolution layers such as those present in the VGG16 network [44]. The decoder consists in semantically projecting the discriminating features learned by the encoder at a lower resolution to a higher resolution. Decoding is nothing more than oversampling. SegNet derives its originality from the way the decoder is applied to switch from a lower to a higher resolution. After that a downsampling operation is performed (max-pooling) at the output of an encoder, and the indices corresponding to the pooling are stored. In other words, the max locations of the encoder feature maps (pooling indices) are stored to perform non-linear upsampling in the decoder network. This technique reduces the number of parameters since it does not need to learn to upsample.

The SegNet network is composed of 13 layers of convolutions (encoders) which correspond to the first 13 layers of the VGG16 (Fig. 2). Each convolution layer is followed by a batch normalization and a non-linear activation function ReLu (Rectified Linear Unit). Batch normalization is used to accelerate deep network training by reducing internal covariate shift [45]. Max-pooling with a 2×2 filter and a stride 2 (no recovery) is applied to the ReLu output. This operation downsamples the input feature map by a factor of 2. Max-pooling makes it possible to reinforce the invariance to translation on small spatial shifts of the input image. However, even if the use of max-pooling is beneficial for translation robustness it causes a loss of spatial resolution

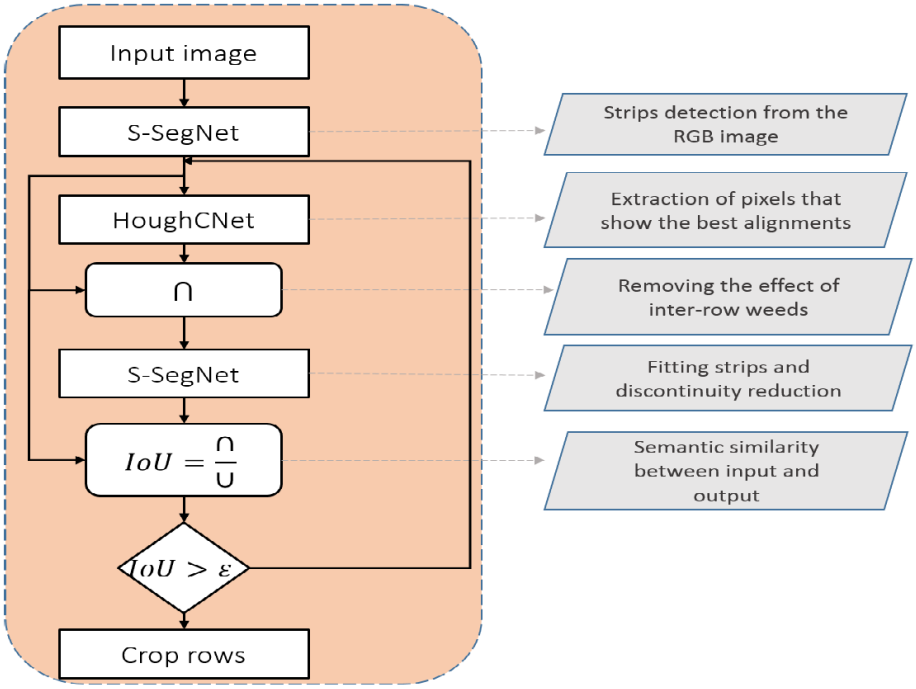

FIGURE 1. Flowchart for crop row detection with CNN (CRowNet).

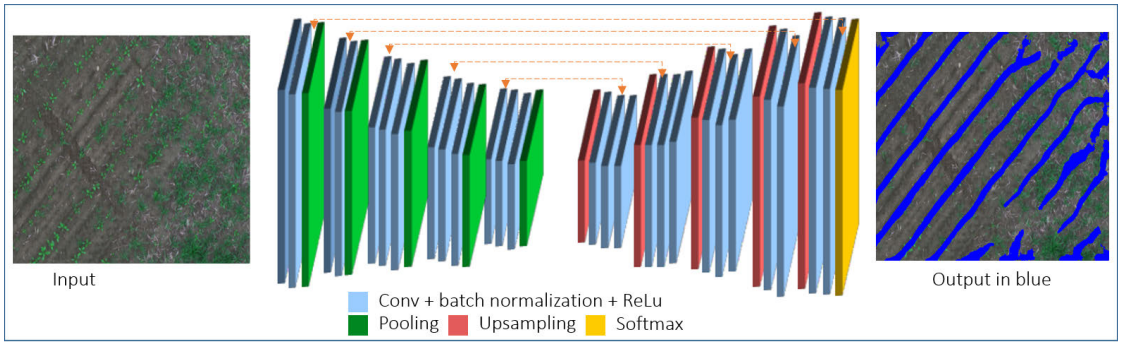

FIGURE 2. Encoder-decoder architecture of SegNet.

which may be less beneficial in applications where boundary delineation is essential. Storing the positions of max values during max-pooling is a good way to deal with this problem. The decoder upsamples the encoder from the stored indices and keeps the number of channels. Therefore, an encoder with 3 channels (RGB) will have 3 channels after encoding; this is the case for the first encoder. The results of oversampling are very sparse, thus a convolution layer followed by a batch normalization is added to produce a map with a denser feature. Finally, the output of the last decoder becomes the input of the Softmax for classification. The K-class softmax classifier is used to predict the class for each pixel, where K corresponds to the number of classes.

B. CNN BASED HOUGH TRANSFORM (HOUGHCNET)

Instead of using superpixels or inter-row distance information to identify the major votes that represent the crop rows, we propose a method that combines the Hough transfrom and CNN. First multiple lines are detected with the Hough transform, then a deep neural network is applied to detect the main lines which correspond to crop rows. The complete process is presented in Fig. 3.

1) HOUGH TRANSFORM

The Hough transform is a pattern recognition technique developed in 1962 by Paul Hough [18], and patented by IBM. This technique, developed more than half a century ago, continues to prove its effectiveness in the field of artificial vision to such an extent that it is considered a standard tool for particular shape detection. It is based on a mechanism of accumulation (vote) from the image space (pixels) to a multidimensional parameter space, called the Hough space. This space simplifies the complex problem of global shape detection. It is useful for the detection of contours that can be

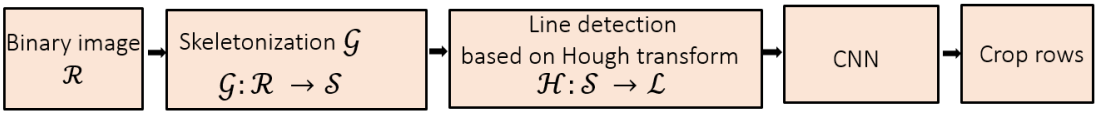

FIGURE 3. Flowchart of the HoughCNet process. As input we have a segmented image and in the output we obtain crop rows after Hough transform and CNN combination.

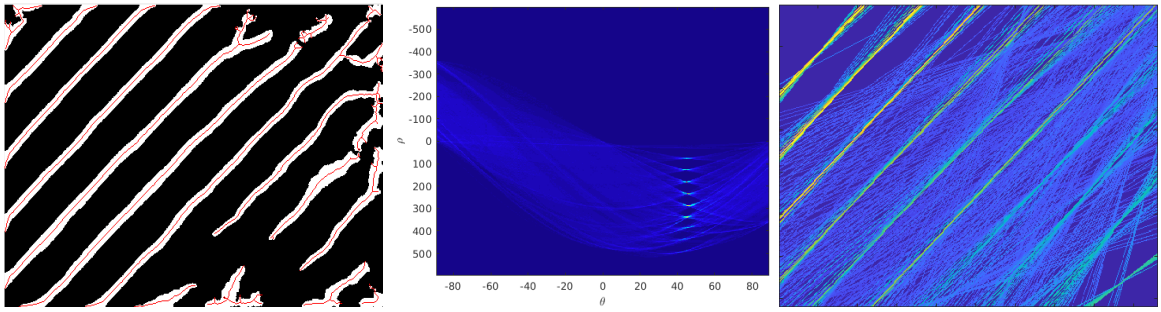

(a) (b) (c)

FIGURE 4. Example of inverse Hough transform result. (a) Binary image in white and its skeleton in red. (b) Hough transform performed in the skeleton. (c) Lines detected with the Hough transform where each line has a value corresponding to its vote in the Hough space ($\mathcal{L}$).

described by few parameters, such as lines, circles, ellipses, etc. In Hough space a line can be represented by the parameters of its cartesian equation (a,b) or polar equation (ρ, θ). Polar parameters are generally preferred, since they can be bounded in very precise intervals, unlike cartesian coordinates (a,b) which can take values from $]-\infty, +\infty[$. The longer a line is in the image space, the more important its vote is in the Hough space. Besides, the Hough transform has a high capacity for joining discontinuous lines.

In principle, a crop row is a succession of several very close lines. Thus, the more plants there are in a crop row, the more time it takes to calculate the Hough transform. To solve the problem of computation time we propose to use the skeletons of the rows. In computer vision, reducing the amount of information to be processed to the minimum necessary has become very important, since it reduces the computation time, contour distortion and some local noise while retaining significant topological and geometric properties. For example the thin-line representation of crop rows is closer to the human conception of these patterns in an agricultural field. Skeletonization is a process that represents a pattern by a collection of thin (or nearly thin) arcs and curves [46]. Depending on the skeletonization method the result can be referred to as *skeleton* or *thinning*. *Skeleton* is used when the result is obtained regardless of the original pattern whereas *thinning* is a line-like representation of the original pattern. The results of the two methods can be quite similar in appearance, which is why the general term used is *skeleton*. In this work, a thinning method was used in order to find the one-pixel mid-lines of crop rows. Iterative thinning is the most widely used method. It is based on removing or keeping successive layers of pixels on the boundary of the pattern until only a skeleton remains [46], [47]. Using only a few pixels, it gives the same information on the geometry of the field: direction of the crop rows, distance between rows and periodicity of the crop rows [27]. Instead of using superpixels or inter-row distance information to identify the major votes which represent the crop rows, we propose a method which combines the Hough transform and CNN. We first computed the normalized Hough transform $H_{norm}(\rho, \theta)$ in order to give the same weight to all the crop rows, especially the short ones close to the borders [8]. Then all the lines are detected ($\mathcal{L}$). The image $\mathcal{L}$ containing the lines of the N peaks of $H_{norm}(\rho, \theta)$ is obtained through (1). Fig. 4 presents an example of this procedure.

Let Ψ_i be an image of the same size as the input image and (X_i, Y_i) the couple of coordinates of all the pixels of Ψ_i (2) belonging to the line represented in $H_{norm}(\rho, \theta)$ by the peak P_i of value α_i.

$$\mathcal{L} = argmax(\Psi_1, \Psi_2, \Psi_3, \ldots, \Psi_N) \quad (1)$$

$$\Psi_i(x, y) = \alpha_i, (x, y) \in (X_i, Y_i) \quad (2)$$

Once $\mathcal{L}$ is obtained, it is used as input of a convolutional neural network to detect crop rows.

2) HOUGHCNET NETWORK

The CNN architecture proposed is composed of 5 convolution layers with dilation. Each convolution layer is composed of 32 filters. Batch normalization and ReLu were applied after each convolution layer. Some authors have shown that dilated convolution is particularly suited to dense prediction due to its ability to expand the receptive field without losing resolution or increasing the number of parameters [48], [49]. The receptive field grows exponentially while the number of parameters grows linearly. A dilated convolution layer is

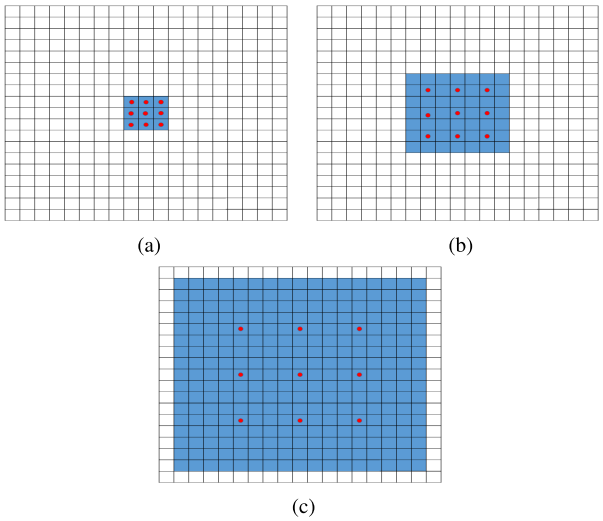

FIGURE 5. Examples of three dilated filters. (a) Filter f_1 used in 1-dilated convolution; each element in f_1 has a receptive field of 3 × 3. (b) Filter f_2 produced from F_1 by 2-dilated convolution; the receptive field for each element is 7 × 7. (c) This filter f_3 is obtained from f_2 by a 4-dilated convolution; the elements in f_3 have a receptive field of 15 × 15. The dilated convolution layers made by the filters have the same number of parameters.

defined as a layer where the convolution is performed with dilated filters (Fig. 5).

The architecture is shown in Fig. 6. Generally in $\mathcal{L}$ each crop row is represented by more than one line, given that we would like to identify those that best go through the center. Thus the first two layers use 4 as dilation values, highlighting the lines that are in the center and conversely reducing the influence of the lines far from the center of the crop rows. These layers are followed by a sub-sampling that keeps the maximum value in a 2 × 2 neighborhood (max pooling) and an oversampling that returns the image to its original size. Then the process is repeated with 2 other convolution layers with 2 as dilation value. The last convolution layer (1 × 1 × 2) is applied, where 2 is the number of classes. Finally, the softmax performs pixel classification (Fig. 6).

IV. RESULTS AND DISCUSSION

The images used come from a public dataset provided by [50]. These images were acquired in a beet field by the Parrot RedEdge-M multispectral sensor 10m from the ground. This public dataset contains 5 subsets of images numbered from 000 to 004. Each subset corresponds to part of the field. For the training, only images in the 003 subset were used and the evaluation was performed on the 000-002 image subsets. The images in subset 004 were not used because of the blurring that was present in some parts of the images. In order to test the robustness of the proposed method, it was applied to images acquired in another field with a different flight altitude and spatial resolution. These new images were acquired in a corn field with Sony camera 100m above the ground with a spatial resolution of 2.5cm. The camera is embedded on Sensefly's fixed-wing UAV eBee.

A. TRAINING

Manual image annotation is very time consuming because it requires not only the ability to draw a continuous line per crop row, but also to repeat the same process for each image. To simplify the annotation process, we proceeded in a semi-supervised manner. The orthomosaic image 003 was divided into patches of 250 × 250 pixels. This size was chosen to obtain images showing crop rows with different layouts (discontinuity, non-regular contours, inter-row weeds, etc.) and also to facilitate the CNN learning. Then we applied CR-Hough-SLIC [27] to detect crop rows in all the image patches. Patches where all crop rows were correctly detected were selected to build the training dataset. The number of learning samples collected was 134. With data augmentation we increased the size of the dataset seven times (Rotation 0°, 45°, 90° and 135° and 3 contrast changes). Fig. 8 presents the dataset used for the training. SegNet was trained with all the training data, while the HoughCNet network was trained only with the original images and data augmented by rotation since samples with contrast change have the same orientation as the original ones.

The ground truth shows that classes are imbalanced: the majority of pixels are in the background and this can affect the learning process. Classes with more trained elements may become more sensitive to identification in relation to classes with fewer trained elements. This class imbalance problem is solved by reweighting the loss by inverse class frequency. Thus the weighting of each class corresponds to the inverse of its frequency in the images. This process has the advantage of increasing the weight of under-represented classes and thus influencing the loss function by assigning a relatively higher weight to the minor classes (Table 1). The difference in weights between S-SegNet and HoughCNet is explained by the fact that the number of samples used is not the same and also because the annotated images used to train S-SegNet are a dilated version of those used for HoughCNet.

TABLE 1. The weights applied for each class and each network.

Networks	Class name	Pixel count	Frequency	Class weights
S-SegNet	line	7441648	0.1269	7.8780
	background	51183352	0.8731	1.1454
HoughCNet	line	2214900	0.0661	15.1248
	background	31285100	0.9339	1.0708

A stochastic gradient descent momentum (SGDM) solver is applied to train the networks. The learning rate is set to 0.001 and the momentum value is 0.9. We used a weighted cross-entropy loss, to handle the imbalanced number of pixels of each class, due to the dominance of the soil. For S-SegNet the number of epochs and mini-batch size are set to 1000 and 4 respectively. As regards HoughCNet the number of epochs and mini-batch size are set to 200 and 20 respectively. The Hough transform $H(\theta, \rho)$ is computed on the $\mathcal{S}$ with a θ resolution equal to 0.1°, letting θ take values in the range $]-90°; 89°]$ and a ρ resolution equal to 1. $\mathcal{S}$ is obtained by using the Matlab *thin* function with $n = Inf$; with this option

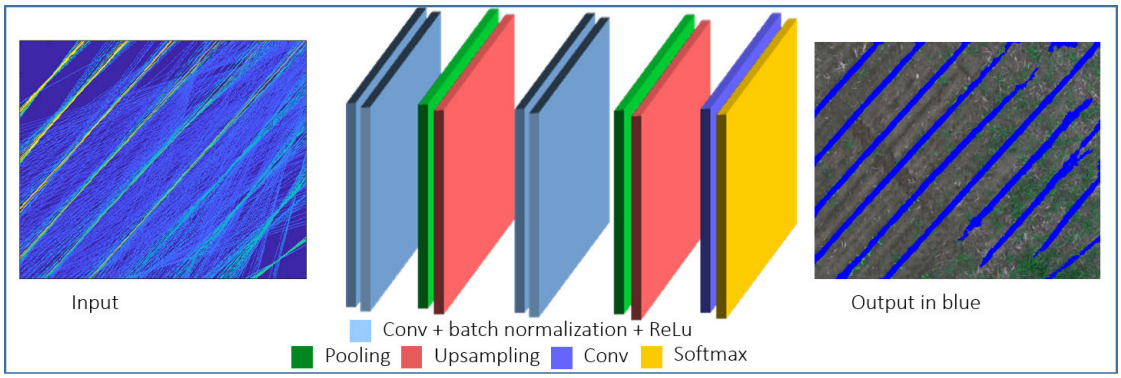

FIGURE 6. Architecture of the HoughCNet network.

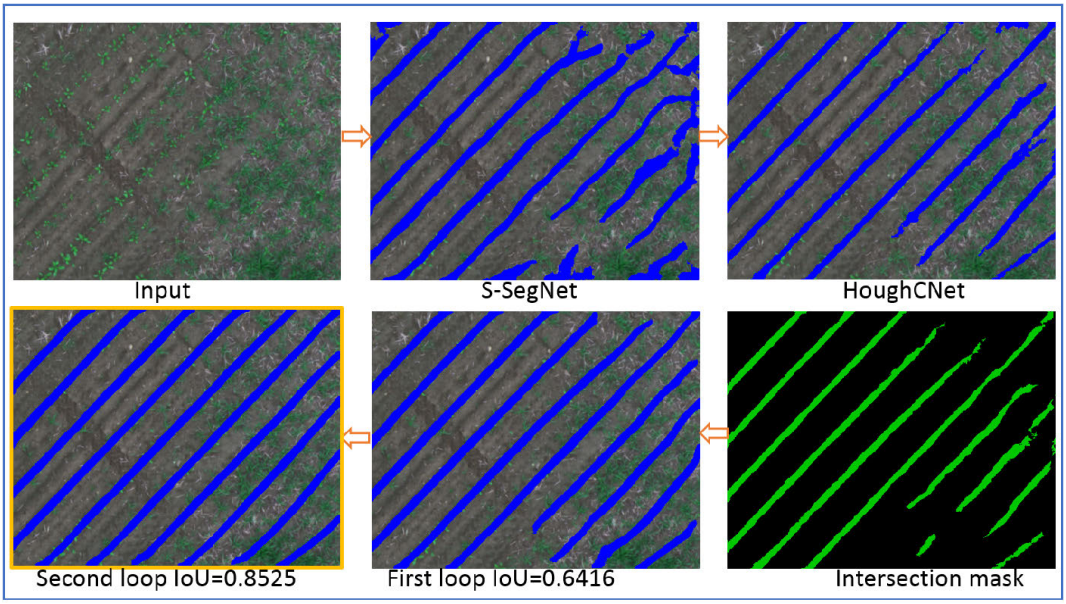

FIGURE 7. Example of crop row detection in a weed-infested image. At the first loop the IoU is 0.6416. After the third loop IoU = 0.8525 and the detected crop rows are more adjusted.

the contour pixels are removed according to the local configuration until the image no longer changes. The CRowNet stop criterion ϵ was set to 0.85. This value of ϵ was considered as a good trade-off between good detection and iteration number.

B. TEST

Assessment was carried out on 154 images (480 × 360 pixels) from datasets number 000, 001 and 002 of the public dataset [50]. In order to take into account crop row irregularities and to avoid the impact of weed pressure in the test data, the ground truth was built manually with the Matlab labeling tool (Image labeler). The labeling consisted in creating a mask around each row. The weed infestation rate (WIR) in these images varies from low to high. The WIR is the proportion of vegetation pixels considered as weeds in an image. According to the WIR classification, we have 45 images without weeds (WIR $<$ 5%), 21 images with a low rate of infestation ([5% - 15%[), 50 images with a moderate infestation rate ([15% - 35%[) and 38 heavily infested (WIR $>$ 35%). These infestation rates were computed from the ground truth of the images available in the public dataset. In total there were 1325 crop rows to detect (N_{CR}).

As for the other images to be used at the input of the network to test its robustness, 80 samples of a maize field were selected; the sample size was 300 × 300 pixels. The total number of crop rows was $N_{CR} = 1081$. This field was chosen because vegetation densities and the spatial resolution are different from the images on which the model was trained. In Fig. 9a it can be seen that the image is affected by plant shadows and the crop rows are difficult to locate even with the naked eye. We therefore performed contrast change by replacing the green channel by the background segmentation result obtained with ExG followed by Otsu thresholding.

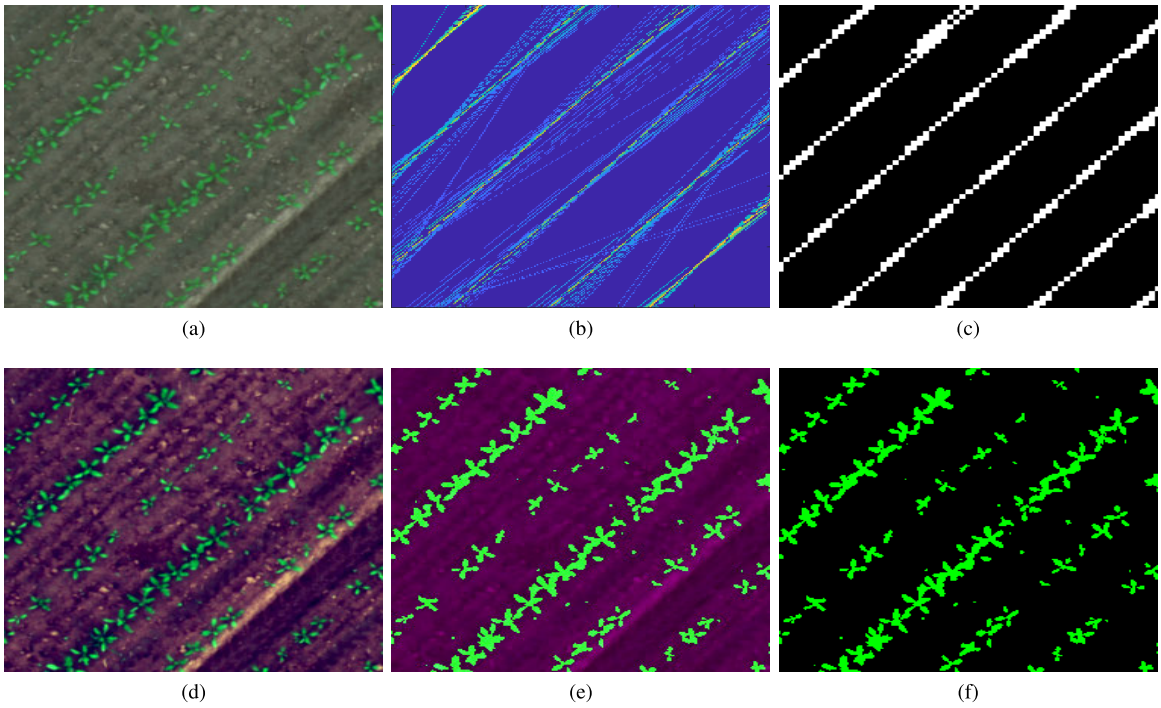

FIGURE 8. Example of the training dataset. (a) The original image X. (b) Line detection based on the Hough transform $\mathcal{L}$. (c) Ground truth. In the second row we have image X after contrast change. (d) Contrast adjustment, the 1 % of pixels are saturated at low and high intensities for each channel of X. (e) The green channel of the RGB image is replaced by the result of background segmentation performed with ExG and Otsu thresholding (BW). (f) Blue and red channels are set to 0 and the green channel corresponds to BW.

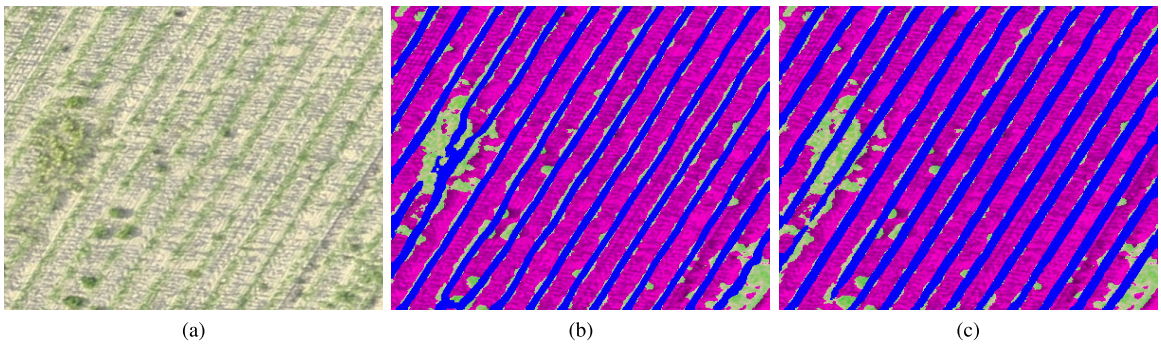

FIGURE 9. Examples of crop row detection on images acquired in the maize field. (a) Original image. (b) Overlay of crop rows detected with S-SegNet (in blue) and the original image after contrast change. (c) Overlay of crop rows detected with CRowNet (in blue) and the original image after contrast change.

1) QUALITATIVE ASSESSMENT

Based on the visual result, a qualitative analysis was performed. In Fig. 9 and 10, it can be seen that S-SegNet is able to locate and represent crop rows with strips even for discontinuous rows, and that crop rows with a low rate of weed infestation in the neighborhood are well detected. Rows which are discontinuous and have weeds in their immediate proximity are detected but with some disturbances. With CRowNet, detection was improved and the impact of weeds was reduced. The other remark that can be made is that the detected strips are mainly located in the center of the crop rows and do not cover all the pixels of the ground truth. This point is normal since models are trained to detect the central alignment. Moreover, Fig. 9 shows that even if all the vegetation has the same value, the method succeeds in detecting all the crop rows.

2) QUANTITATIVE ASSESSMENT

Four metrics were computed for performance evaluation: the recall (Recall), the precision (Precision), the F_1 score and the intersection over the union (IoU). Recall reflects the ability to reveal the needed information (3), Precision (4) indicates the correctness of the detected results, and the F_1 score indicates the balance between Precision and Recall (5). It is the harmonic mean of precision and recall. These indices were computed for each crop row. In addition, to assess how

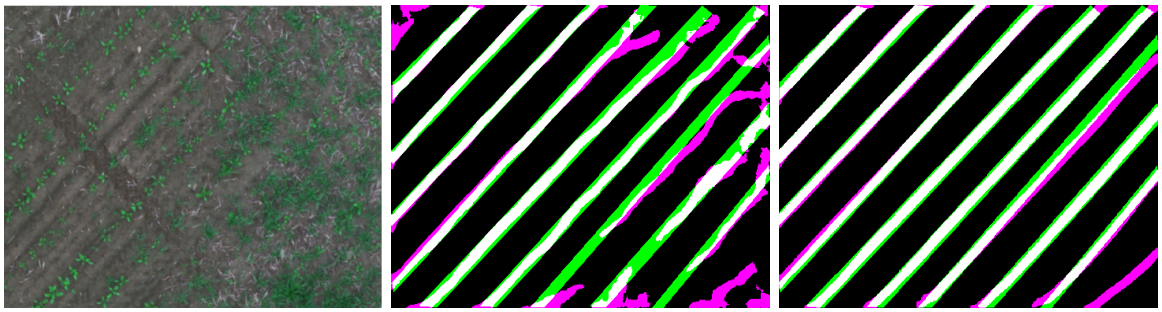

(a) (b) (c)

FIGURE 10. Crop row detection using S-SegNet and CRowNet. (a) Original RGB image. (b) and (c) are the results of S-SegNet and CRowNet respectively. The white color represents the ground truth pixels that are well detected (true positive), in magenta the pixels that are on the predicted row and that do not belong to the ground truth (false positive), and in green the missed pixels (false negative).

accurate the method is in each image and row we computed the intersection over union metric (IoU). IoU, also called the Jaccard similarity coefficient (6) takes into account both the false alarms and the missed values for each class. The IoU is calculated as a ratio of the area of overlap to the area of the union between ground truth (GT) and the prediction. The recall, precision and F_1 score were calculated for each crop row to measure the effectiveness of each individual detection. In addition, the IoU was computed for each image, thus making it possible to assess the impact of overdetection in each image. The number of crop rows in a field can sometimes be considered as an indicator of good plant growth and good yield. Consequently, a curve of good detection rate (GDR) of crop rows according to the segmentation quality (τ) required for the IoU score is plotted (7).

$$Recall = \frac{TP}{TP + FN} \tag{3}$$

$$Precision = \frac{TP}{TP + FP} \tag{4}$$

$$F_1 = \frac{2 \times Recall \times Precision}{Precision + Recall} \tag{5}$$

$$IoU = \frac{GT \cap P}{GT \cup P} \tag{6}$$

$$GDR = \frac{Card(IoU \geq \tau)}{N_{CR}} \tag{7}$$

True positives (TPs) are pixels that are correctly detected as belonging to a crop row while false positives (FPs) are pixels misclassified as belonging to crop row. Finally, false negatives (FNs) are pixels belonging to a crop row but detected as background, and true negatives (TNs) are background pixels detected as pixels of a crop row. As a reminder N_{CR} represents the number of crop rows to be detected in the field.

Table 2 shows that the results of S-SegNet and CRowNet are close. CRowNet generally outperforms when S-SegNet provides discontinuous crop rows. With CRowNet each row is detected on average with a Recall of 70.72% and a Precision of 90.10%. The qualitative assessment carried out is well reflected in the quantitative assessment. Results are explained by the position of rows detected according to the ground truth.

TABLE 2. Quantitative results of crop row detection in the beet field. The mean is computed for each row.

Method	Mean Recall	Mean Precision	Mean F_1	Mean IoU
S-SegNet	0.6614	0.8981	0.7472	0.60081
CRowNet	0.7072	0.9010	0.7794	0.6486

To efficiently evaluate the results, we thinned all the rows and each row was represented by its skeleton. Assuming that the thinning operation returns skeletons which represent the center line of each row, we dilated the skeletons to obtain the same crop row width as that measured in the field. Based on a ground measurement in the beet field, the size of a crop plant varies from 15 to 20 pixels. In the maize field the crop row width is about 12 pixels. We therefore dilated the skeleton of detected rows with a square structuring element of 15 $\times$ 15 pixels on beet images and 11 $\times$ 11 pixels on maize images. Fig. 11a and 11b present the results of the thinning and those of dilation. CRowNet was compared to different semantic segmentation methods including SegNet with imbalanced classes, FCN [51], FCN-W and FCN-W-16. FCN-W and FCN-W-16 are respectively FCN-8s and FCN-16s with balanced classes.

Besides semantic segmentation methods, we compared CRowNet with two other methods proposed in the literature. The most commonly used methods for detecting crop rows in aerial images use the Hough transform and geometric field information (inter-row distance, global orientation, etc.). Depending on the authors, the Hough transform is applied to all vegetation pixels [8], [24], or to the centroids of plants [25], but the fundamental principle remains the same. First the Hough transform is computed, then the peak of the majority vote is identified. From the position of this peak and the estimated inter-row distance, other peaks are identified. This method assumes that in images without perspective, crop rows are parallel with a constant inter-row distance; in the rest of this article, this approach will be called CR-Hough. We compared CRowNet with CR-Hough and CR-Hough-SLIC. To compute these two methods, a background segmentation was performed with ExG and Otsu thresholding.

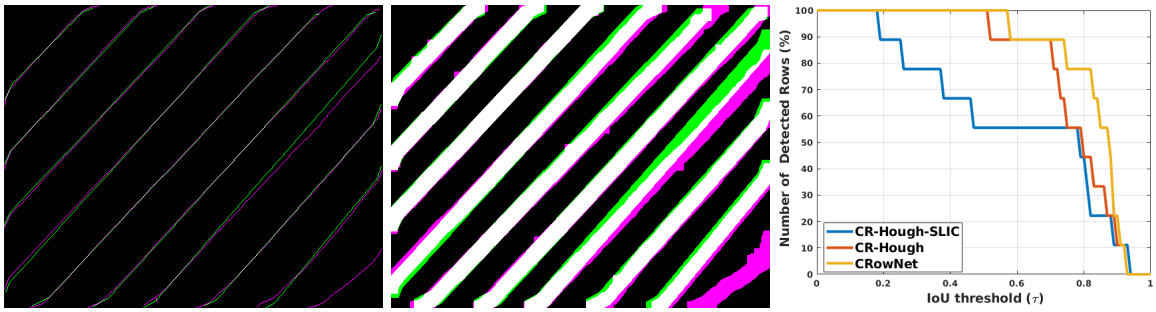

FIGURE 11. (a) and (b) are respectively the results of CRowNet after skeletization and dilation of the skeletons. The white color corresponds to the true positives (TPs), magenta corresponds to the false positives (FPs), and green to the false negatives (FNs). (c) Number of detected crop rows according to the segmentation quality. CR-Hough is the result obtained with the Hough transform and field information [8], [24]. CR-Hough-SLIC is the result obtained with the combination of the Hough transform and SLIC [27].

TABLE 3. Results of crop row detection methods after performing a dilation. FCN-W and FCN-W-16 are respectively FCN-8s and FCN-16s with balanced classes.

Data	Method	Mean Recall	Mean Precision	Mean F-score	Mean IoU	Mean IoU/image
Beet	SegNet	0.6740	0.8024	0.7179	0.6350	0.7650
	FCN	0.2625	0.4969	0.3215	0.2135	0.2839
	FCN-W	0.6512	0.6442	0.6318	0.4924	0.4984
	FCN-W-16	0.6544	0.6635	0.6442	0.5063	0.5111
	CRowNet	**0.9056**	0.9037	**0.9039**	**0.8319**	**0.7896**
	CR-Hough-SLIC	0.8567	0.8658	0.8540	0.7660	0.7492
	CR-Hough	0.8687	**0.9094**	0.8876	0.8027	0.7299
Maize	**CRowNet**	**0.8093**	0.8457	**0.8250**	**0.7572**	0.8280
	CR-Hough-SLIC	0.7974	**0.8514**	0.8213	0.7516	**0.8290**
	CR-Hough	0.7907	0.8438	0.8149	0.7407	0.8154

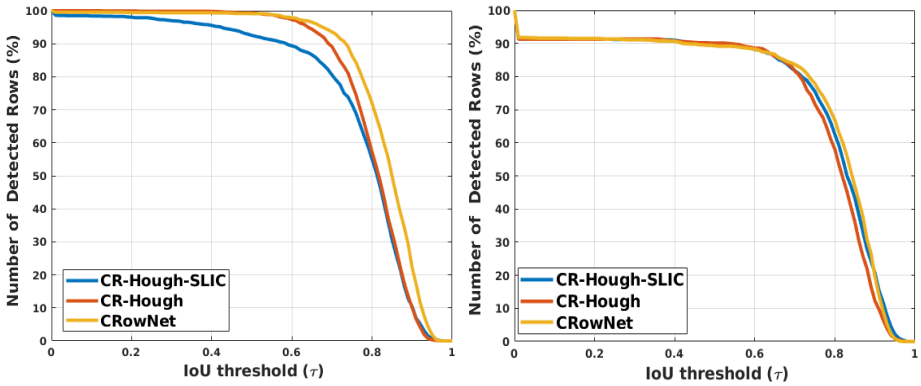

FIGURE 12. Well detected crop rows depending on the quality of the segmentation. (a) and (b) present results obtained with data taken in the beet and in maize fields.

On beet images for CR-Hough, the theoretical value used is 45° for the global orientation, the inter-row distance estimated is 50 pixels and the row width is 20. On maize images, the estimated global orientation, inter-row distance and row width are respectively 29°, 22 and 12. The number of superpixels applied to compute CR-Hough-SLIC in beet and maize images are respectively 0.1% and 0.5% of the pixels present in the image.

The result of the comparison is shown in Table 3. It can be seen that CRowNet provides the best results. It outperforms all the other methods in the beet field and the results obtained with the different versions of FCN provide the lowest results. The F1 score and the Precision of CRowNet and CR-Hough are close but the difference is greater when looking at the IoU per image. The result of the IoU for CR-Hough shows that CR-Hough overdetects more than the other two methods (CR-Hough-SLIC and CRowNet). This overdetection is greater on images with a high weed infestation rate. Table 4 shows how the weed pressure influences the results. CRowNet is more robust and we remark that the higher the WIR, the higher the performance gap between CRowNet and these two methods. It is also noted in Table 3 that CRowNet trained in the beet

TABLE 4. Mean IoU results according to the weed infestation rate on images acquired in the beet field.

Method	Low	Moderate	High
CRowNet	**0.8449**	**0.8026**	**0.7239**
CR-Hough-SLIC	0.7986	0.7971	0.6387
CR-Hough	0.7903	0.7474	0.6513

field gives results comparable to those of CR-Hough and CR-Hough-SLIC in the maize field.

Fig. 11c and 12 show the performance of the methods according to the IoU obtained in each crop row. We note that due to the irregularity of the crop rows shape, it is difficult to obtain a 100% overlay between the ground truth and the prediction. In addition, it can be seen in Fig. 12a that for a value of $\tau = 0.70$, the number of rows that are well detected with CRowNet is 93.58%. In the maize field, the quality of the segmentation is close and this is highlighted in Fig. 12b and Table 3. It can also be seen that the CR-Hough-SLIC method outperforms the CRowNet for high values of IoU threshold. However, compared to CR-Hough and CR-Hough-SLIC, CRowNet does not need theoretical field information and has no adjustable parameters.

V. CONCLUSION

In this article, we have proposed a new automatic method for detecting crop rows. This method called CRowNet combines CNN and the Hough transform and consists of a model formed with S-SegNet and a CNN based on the Hough transform (HoughCNet). The model was evaluated in two different fields: a beet field on which part of the images was used to train the models and a maize field with a different spatial resolution to test the robustness of the generated model. The results obtained show that it is possible to detect crop rows with a convolutional neural network even with a high weed pressure. In addition to semantic segmentation methods, CRowNet was also compared with methods without training and that are based on the Hough transform (CR-Hough and CR-Hough-SLIC). The IoU scores obtained with CRowNet outperformed the ones achieved with other methods in both fields. In the images acquired in the beet field, 93.58% of crop rows were detected with an IoU score above 70%. CRowNet also demonstrated its robustness in a maize field with a strong presence of shadows after contrast change. In addition, in contrast to methods found in the literature, CRowNet does not require field information or calibration of superpixels. As future work, we plan to replace CRowNet with only one CNN model.

REFERENCES

[1] European Crop Protection. (2017). *With or Without Pesticides? | ECPA*. Accessed: Feb. 20, 2017. [Online]. Available: http://www.ecpa.eu/with-or-without

[2] F. J. Pierce and P. Nowak, "Aspects of precision agriculture," *Adv. Agronomy*, vol. 67, pp. 1–85, May 1999.

[3] A. Mcbratney, B. Whelan, T. Ancev, and J. Bouma, "Future directions of precision agriculture," *Precis. Agricult.*, vol. 6, no. 1, pp. 7–23, 2005.

[4] D. J. Mulla, "Twenty five years of remote sensing in precision agriculture: Key advances and remaining knowledge gaps," *Biosyst. Eng.*, vol. 114, no. 4, pp. 358–371, Apr. 2013.

[5] W. Winterhalter, F. V. Fleckenstein, C. Dornhege, and W. Burgard, "Crop row detection on tiny plants with the pattern Hough transform," *IEEE Robot. Autom. Lett.*, vol. 3, no. 4, pp. 3394–3401, Oct. 2018.

[6] X. P. Burgos-Artizzu, A. Ribeiro, M. Guijarro, and G. Pajares, "Real-time image processing for crop/weed discrimination in maize fields," *Comput. Electron. Agricult.*, vol. 75, no. 2, pp. 337–346, 2011.

[7] F. Rovira-Más, Q. Zhang, J. Reid, and J. Will, "Hough-transform-based vision algorithm for crop row detection of an automated agricultural vehicle," *Proc. Inst. Mech. Eng., D, J. Automobile Eng.*, vol. 219, no. 8, pp. 999–1010, 2005.

[8] C. Gée, J. Bossu, G. Jones, and F. Truchetet, "Crop/weed discrimination in perspective agronomic images," *Comput. Electron. Agricult.*, vol. 60, no. 1, pp. 49–59, 2008.

[9] J. M. Peña, J. Torres-Sánchez, A. I. De Castro, M. Kelly, and F. López-Granados, "Weed mapping in early-season maize fields using object-based analysis of unmanned aerial vehicle (UAV) images," *PLoS ONE*, vol. 8, no. 10, 2013, Art. no. e77151.

[10] Y. LeCun, L. Bottou, Y. Bengio, and P. Haffner, "Gradient-based learning applied to document recognition," *Proc. IEEE*, vol. 86, no. 11, pp. 2278–2323, Nov. 1998.

[11] A. Krizhevsky, I. Sutskever, and G. E. Hinton, "ImageNet classification with deep convolutional neural networks," in *Proc. Adv. Neural Inf. Process. Syst.*, 2012, pp. 1–9.

[12] M. Bah, A. Hafiane, and R. Canals, "Deep learning with unsupervised data labeling for weed detection in line crops in UAV images," *Remote Sens.*, vol. 10, no. 11, p. 1690, 2018.

[13] M. D. Bah, E. Dericquebourg, A. Hafiane, and R. Canals, "Deep learning based classification system for identifying weeds using high-resolution UAV imagery," in *Proc. Comput. Conf.*, 2018.

[14] A. Kamilaris and F. X. Prenafeta-Boldú, "Deep learning in agriculture: A survey," *Comput. Electron. Agricult.*, vol. 147, pp. 70–90, Apr. 2018.

[15] M. Kerkech, A. Hafiane, and R. Canals, "Deep leaning approach with colorimetric spaces and vegetation indices for vine diseases detection in UAV images," *Comput. Electron. Agricult.*, vol. 155, pp. 237–243, Dec. 2018.

[16] A. K. Mortensen, M. Dyrmann, H. Karstoft, R. N. Jørgensen, and R. Gislum, "Semantic segmentation of mixed crops using deep convolutional neural network," in *Proc. CIGR-AgEng Conf.*, 2016.

[17] C. Hung, Z. Xu, and S. Sukkarieh, "Feature learning based approach for weed classification using high resolution aerial images from a digital camera mounted on a UAV," *Remote Sens.*, vol. 6, no. 12, pp. 12037–12054, Dec. 2014.

[18] P. V. C. Hough, "Method and means for recognizing complex patterns," U.S. Patent 3 069 654 A, Dec. 18, 1962.

[19] B. Åstrand and A.-J. Baerveldt, "A vision based row-following system for agricultural field machinery," *Mechatronics*, vol. 15, no. 2, pp. 251–269, 2005.

[20] V. Leemans and M. F. Destain, "Line cluster detection using a variant of the Hough transform for culture row localisation," *Image Vis. Comput.*, vol. 24, no. 5, pp. 541–550, 2006.

[21] T. Bakker, H. Wouters, K. van Asselt, J. Bontsema, L. Tang, J. Müller, and G. van Straten, "A vision based row detection system for sugar beet," *Comput. Electron. Agricult.*, vol. 60, no. 1, pp. 87–95, 2008.

[22] D. M. Woebbecke, G. E. Meyer, K. Von Bargen, and D. A. Mortensen, "Color indices for weed identification under various soil, residue, and lighting conditions," *Trans. ASAE*, vol. 38, no. 1, pp. 259–269, 1995.

[23] N. Otsu, "A threshold selection method from gray-level histograms," *IEEE Trans. Syst., Man, Cybern.*, vol. SMC-9, no. 1, pp. 62–66, Jan. 1979.

[24] G. Jones, C. Gée, and F. Truchetet, "Modelling agronomic images for weed detection and comparison of crop/weed discrimination algorithm performance," *Precis. Agricult.*, vol. 10, no. 1, pp. 1–15, 2009.

[25] R. Ji and L. Qi, "Crop-row detection algorithm based on random Hough transformation," *Math. Comput. Model.*, vol. 54, pp. 1016–1020, Aug. 2011.

[26] L. Xu and E. Oja, "Randomized Hough transform (RHT): Basic mechanisms, algorithms, and computational complexities," *Comput. Vis., Graph., Image Process., Image Understand.*, vol. 57, no. 2, pp. 131–154, 1993.

[27] M. D. Bah, A. Hafiane, and R. Canals, "Weeds detection in UAV imagery using SLIC and the Hough transform," in *Proc. 7th Int. Conf. Image Process. Theory, Tools Appl. (IPTA)*, Nov. 2017, pp. 1–6.

[28] H. T. Søgaard and H. J. Olsen, "Determination of crop rows by image analysis without segmentation," *Comput. Electron. Agricult.*, vol. 38, no. 2, pp. 141–158, Feb. 2003.
[29] T. Hague, N. D. Tillett, and H. Wheeler, "Automated crop and weed monitoring in widely spaced cereals," *Precis. Agricult.*, vol. 7, no. 1, pp. 21–32, 2006.
[30] S. J. Julier and J. K. Uhlmann, "Unscented filtering and nonlinear estimation," *Proc. IEEE*, vol. 92, no. 3, pp. 401–422, Mar. 2004.
[31] M. Montalvo, G. Pajares, J. M. Guerrero, J. Romeo, M. Guijarro, A. Ribeiro, J. J. Ruz, and J. M. Cruz, "Automatic detection of crop rows in maize fields with high weeds pressure," *Expert Syst. Appl.*, vol. 39, no. 15, pp. 11889–11897, 2012.
[32] V. Fontaine, and T. G. Crowe, "Development of line-detection algorithms for local positioning in densely seeded crops," *Can. Biosyst. Eng.*, 2006, vol. 48, p. 7.
[33] M. Kise, Q. Zhang, and F. R. Más, "A stereovision-based crop row detection method for tractor-automated guidance," *Biosyst. Eng.*, vol. 90, no. 4, pp. 357–367, 2005.
[34] F. Rovira-Más, Q. Zhang, and J. F. Reid, "Stereo vision three-dimensional terrain maps for precision agriculture," *Comput. Electron. Agricult.*, vol. 60, no. 2, pp. 133–143, 2008.
[35] A. Milioto, P. Lottes, and C. Stachniss, "Real-time blob-wise sugar beets vs weeds classification for monitoring fields using convolutional neural networks," *Ann. Photogramm., Remote Sens. Spatial Inf. Sci.*, vol. IV-2/W3, pp. 41–48, Sep. 2017.
[36] A. dos Santos Ferreira, D. M. Freitas, G. G. da Silva, H. Pistori, and M. T. Folhes, "Weed detection in soybean crops using ConvNets," *Comput. Electron. Agricult.*, vol. 143, pp. 314–324, Dec. 2017.
[37] X. Pan, J. Shi, P. Luo, X. Wang, and X. Tang, "Spatial as deep: Spatial CNN for traffic scene understanding," in *Proc. 32nd AAAI Conf. Artif. Intell.*, 2018.
[38] F. Visin, K. Kastner, K. Cho, M. Matteucci, A. Courville, and Y. Bengio, "ReNet: A recurrent neural network based alternative to convolutional networks," 2015, *arXiv:1505.00393*. [Online]. Available: https://arxiv.org/abs/1505.00393
[39] S. Bell, C. Lawrence Zitnick, K. Bala, and R. Girshick, "Inside-outside net: Detecting objects in context with skip pooling and recurrent neural networks," in *Proc. IEEE Conf. Comput. Vis. Pattern Recognit. (CVPR)*, Jun. 2016, pp. 2874–2883.
[40] G. Qu, W. Zhang, Z. Wang, X. Dai, J. Shi, J. He, F. Li, X. Zhang, and Y. Qiao, "Stripnet: Towards topology consistent strip structure segmentation," in *Proc. ACM Multimedia Conf.*, 2018, pp. 283–291.
[41] S. Lee, J. Kim, J. Shin Yoon, S. Shin, O. Bailo, N. Kim, T.-H. Lee, H. S. Hong, S.-H. Han, and I. S. Kweon, "VPGNet: Vanishing point guided network for lane and road marking detection and recognition," in *Proc. IEEE Int. Conf. Comput. Vis.*, Oct. 2017, pp. 1947–1955.
[42] L. Geng, J. Sun, Z. Xiao, F. Zhang, and J. Wu, "Combining CNN and MRF for road detection," *Comput. Elect. Eng.*, vol. 70, pp. 895–903, Aug. 2018.
[43] V. Badrinarayanan, A. Kendall, and R. Cipolla, "SegNet: A deep convolutional encoder-decoder architecture for image segmentation," *IEEE Trans. Pattern Anal. Mach. Intell.*, vol. 39, no. 12, pp. 2481–2495, Dec. 2017.
[44] K. Simonyan and A. Zisserman, "Very deep convolutional networks for large-scale image recognition," 2015, pp. 1–14, *arXiv:1409.1556*. [Online]. Available: https://arxiv.org/abs/1409.1556
[45] S. Ioffe and C. Szegedy, "Batch normalization: Accelerating deep network training by reducing internal covariate shift," 2015, *arXiv:1502.03167*. [Online]. Available: https://arxiv.org/abs/1502.03167
[46] L. Lam, S.-W. Lee, and C. Y. Suen, "Thinning methodologies-a comprehensive survey," *IEEE Trans. Pattern Anal. Mach. Intell.*, vol. 14, no. 9, pp. 869–885, Sep. 1992.
[47] B. Bataineh, "An iterative thinning algorithm for binary images based on sequential and parallel approaches," *Pattern Recognit. Image Anal.*, vol. 28, no. 1, pp. 34–43, 2018.
[48] F. Yu and V. Koltun, "Multi-scale context aggregation by dilated convolutions," 2015, *arXiv:1511.07122*. [Online]. Available: https://arxiv.org/abs/1511.07122
[49] R. Hamaguchi, A. Fujita, K. Nemoto, T. Imaizumi, and S. Hikosaka, "Effective use of dilated convolutions for segmenting small object instances in remote sensing imagery," in *Proc. IEEE Winter Conf. Appl. Comput. Vis. (WACV)*, Mar. 2018, pp. 1442–1450.
[50] I. Sa, M. Popović, R. Khanna, Z. Chen, P. Lottes, F. Liebisch, J. Nieto, C. Stachniss, A. Walter, and R. Siegwart, "Weedmap: A large-scale semantic weed mapping framework using aerial multispectral imaging and deep neural network for precision farming," *Remote Sens.*, vol. 10, no. 9, p. 1423, 2018.
[51] J. Long, E. Shelhamer, and T. Darrell, "Fully convolutional networks for semantic segmentation," in *Proc. IEEE Conf. Comput. Vis. Pattern Recognit.*, Jun. 2015, pp. 3431–3440.

MAMADOU DIAN BAH received the M.S. degree in electronics, electrotechnics, automatics (EEA) from the University of Toulouse III (Paul Sabatier), France, in 2015, and the M.S. degree in geomatics from the National Institute of Agronomy of Toulouse (ENSAT), in 2016. He is currently pursuing the Ph.D. degree with the University of Orléans, France. He is also a Temporary Lecturer and also a Research Assistant with the University of Orléans. His research interests include image processing, machine learning, and their application for weed detection in agricultural field using unmanned aerial images.

ADEL HAFIANE received the M.S. degree in embedded systems and information processing and the Ph.D. degree from the University of Paris-Sud, in 2002 and 2005, respectively. After that, he worked one year in teaching and research at Paris-Sud, and later for one year at the INSA Centre Val de Loire (INSA CVL) (Former ENSI de Bourges). He was Postdoctoral Fellow at the Computer Science Department, University of Missouri, from 2007 to 2008. He has been with the INSA CVL, since September 2008. He is a member of the Images and Vision Group, PRISME Laboratory, University of Orléans-INSA CVL. He was also an Invited Researcher at the University of Missouri on multiple periods, from 2009 to 2013. He is currently an Associate Professor with INSA CVL. His research interests include theory and methods of image processing, computer vision and machine learning for many applications medical, agriculture, and robotics.

RAPHAEL CANALS received the Dipl.Ing. degree in electrical engineering and the Ph.D. degree in electronics from the University of Clermont-Ferrand, France, in 1989 and 1993, respectively. In 1993, he was Postdoctoral Fellow at the Computer Science Department, CNRC, Ottawa, ON, Canada. In 1994, he joined the Polytechnic School, University of Orléans, France, as a Teacher. He is currently a Researcher with Laboratory PRISME, University of Orléans-INSA CVL. He is also an Associate Professor with the University of Orléans. In 2015, he was introduced at the AgreenTech Valley Cluster dedicated to digital technologies for plant industry. His current interests are in biomedical imaging, innovation for agriculture, the IoT, and AI.